

## Article

# The Influence of Nanostructured Alumina Coating on Bonding and Optical Properties of Translucent Zirconia Ceramics: In Vitro Evaluation

Tine Malgaj <sup>1,\*</sup>,<sup>†</sup> , Tadej Mirt <sup>1,†</sup> , Andraž Kocjan <sup>2</sup>  and Peter Jevnikar <sup>1</sup> 

<sup>1</sup> Department of Prosthodontics, Faculty of Medicine, University of Ljubljana, Hrvatski trg 6, 1000 Ljubljana, Slovenia; tadej.mirt@mf.uni-lj.si (T.M.); peter.jevnikar@mf.uni-lj.si (P.J.)

<sup>2</sup> Department for Nanostructured Materials, Jožef Stefan Institute, Jamova 39, 1000 Ljubljana, Slovenia; a.kocjan@ijs.si

\* Correspondence: tine.malgaj@mf.uni-lj.si; Tel.: +386-31-410-140

† Both authors contributed equally to this work.

**Abstract:** Thin, non-retentive, monolithic restorations fabricated from novel translucent zirconia ceramics are widely used in contemporary dentistry. Because of the chemical inertness of zirconia, debonding of such restorations remains the main clinical complication. Limited evidence on the bonding performance of novel translucent zirconia exists; therefore, the present study aimed to evaluate, *in vitro*, the shear-bond strength (SBS) of translucent zirconia modified with a nanostructured alumina coating (NAC). The SBS of resin cement to translucent zirconia, materials containing 3, 4 or 5 mol.% of yttria modified with NAC, was measured and related to airborne-particle abraded (APA) zirconia surfaces. Half of each of the specimen groups ( $n = 20$ ) were subjected to 37,500 thermocycles in water. In addition, to evaluate the effect of NAC on thin translucent zirconia discs ( $n = 10$ ), the translucency parameter (TP) was measured and compared with APA. The results were statistically analyzed using a *t*-test and one-way ANOVA. NAC provided higher resin-zirconia SBS compared to APA, not affecting the zirconia optical properties. APA, on the other hand, lowered TP for all types of zirconia. NAC did not impair the mechanical or optical properties of translucent zirconia materials and should be regarded as a zirconia pretreatment alternative to APA.

**Keywords:** translucent zirconia; nanostructured alumina coating; airborne-particle abrasion; shear-bond strength; translucency parameter



**Citation:** Malgaj, T.; Mirt, T.; Kocjan, A.; Jevnikar, P. The Influence of Nanostructured Alumina Coating on Bonding and Optical Properties of Translucent Zirconia Ceramics: In Vitro Evaluation. *Coatings* **2021**, *11*, 1126. <https://doi.org/10.3390/coatings11091126>

Academic Editor: Csaba Balázs

Received: 14 August 2021

Accepted: 14 September 2021

Published: 16 September 2021

**Publisher's Note:** MDPI stays neutral with regard to jurisdictional claims in published maps and institutional affiliations.



**Copyright:** © 2021 by the authors. Licensee MDPI, Basel, Switzerland. This article is an open access article distributed under the terms and conditions of the Creative Commons Attribution (CC BY) license (<https://creativecommons.org/licenses/by/4.0/>).

## 1. Introduction

Zirconia ceramic materials are increasingly used in contemporary dentistry given its biocompatibility, exceptional mechanical properties, and pleasing esthetics [1]. However, because of its inferior optical properties and opaque appearance, the indications of conventional 3 mol.% yttria-stabilized (3Y-TZP) zirconia are limited mainly to framework materials for crowns, fixed partial dentures, and implant abutments [2–4]. Recently, novel translucent zirconia generations with increased yttria molar concentration of 4% or 5% were introduced. These increased yttria concentrations promoted the formation of a cubic crystal lattice that reduced light scattering and enhanced the translucency of the material [5]. This, more esthetic, zirconia can now be successfully employed for the fabrication of thin monolithic restorations widely used in minimally invasive dentistry. This rehabilitation presents a well-established treatment modality in contemporary prosthodontics, since only minimal tooth preparation is required [6]. While these restorations offer only a limited bonding surface, a strong and durable resin-bond to the zirconia bonding surface is of utmost importance to achieve long-term success [6]. However, due to the increased chemical stability of zirconia ceramics, debonding remains the main clinical complication, especially in cases of completely non-retentive restorations [7,8]. Various zirconia pretreatment methods have, therefore, been proposed [9–16].

To improve micromechanical interlocking and increase zirconia bonding surface area, airborne-particle abrasion (APA) combined with primer, or cement, containing phosphate adhesive monomer—which promotes chemical bonds to oxide-ceramics—has commonly been advocated [6,17,18]. However, it has been shown that APA can lead to zirconia strength degradation and premature failures, as it introduces surface cracks and plastic deformations [19–23]. In addition, microstructural modifications of translucent zirconia, such as increased yttria content and decreased alumina content, may negatively impact the mechanical properties of this material [24]. It has been shown that zirconia with an increased yttria content of 5 mol.% is more susceptible to APA's damaging effect due to its absence of a tetragonal-to-monoclinic toughening mechanism [25]. Furthermore, zirconia surface changes resulting from APA may lead to lowered translucency, thus impairing the optical properties of thin zirconia restorations.

Non-invasive pretreatment with a nanostructured alumina coating (NAC) to enhance the resin-zirconia bond has recently been proposed. NAC produces a several hundred nm thin alumina layer of lamellar-like topography that provides a higher resin bond to conventional 3Y-TZP zirconia ceramics than APA [26–28]. Furthermore, the coating application provides added nano-roughening of the ceramic surface, thus not promoting any surface flaws or stresses that could impair the strength of the ceramic. NAC's clinical efficiency and compliance with routine dental procedures has also been confirmed [29,30]. However, neither the influence of NAC on the resin bond strength to novel zirconia generations, or NAC's effect on material translucency, has been evaluated as of yet.

In order to advocate NAC as a promising, nondamaging, alternative for pretreating thin translucent zirconia restorations in a manner that does not interfere with the material's mechanical and optical properties, further studies are needed. Therefore, the present study aimed to evaluate the effect of NAC on resin bond strength to novel translucent zirconia and assess the influence of NAC on zirconia translucency. The null hypotheses were as follows: (1) different types of zirconia ceramics and pretreatment methods have no influence on the resin-zirconia bond; (2) APA and NAC have no influence on the translucency of different types of zirconia ceramics.

## 2. Materials and Methods

### 2.1. Specimen Preparation

Three different zirconia ceramic substrates were fabricated from three, commercially available, ready-to-press, and biomedical-grade granulated zirconia powders containing 3 mol.% (TZ-PX-242A, Tosoh, Tokyo, Japan), 4 mol.% (Zpex4, Tosoh, Tokyo, Japan), and 5 mol.% (ZpexSmile, Tosoh, Tokyo, Japan) of yttria in solid solutions. The TZ-PX-242A, Zpex4, and ZpexSmile powders contained 0.05 wt.% of added alumina and about 3 wt.% of inorganic binder. The resulting ceramic powders are referred to as 3Y, 4Y, and 5Y throughout the text, respectively. Uniaxial dry pressing, in a floating die, at 147 MPa with a dwell time of 30 s (PW 10, P/O/Weber, Remshalden, Germany) was used to shape disc pellets that were 20 mm in diameter and 4 mm thick for the shear bond strength testing, and 1.3 mm thick for the translucency measurements. They were then pressure-less sintered at 1450 °C for 2 h, in accordance with the powder supplier's recommendations. Relative density was measured according to Archimedes' method using deionized water as the immersion liquid. All materials reached approximate levels of theoretical density.

According to the experimental protocol (Figure 1), disc-shaped specimens for each of the three types of zirconia (3Y, 4Y, 5Y) were produced and randomly divided into 3 groups of 20; for the shear bond strength testing, and 10 for translucency measurements. The groups were subjected to the following pretreatment conditions:

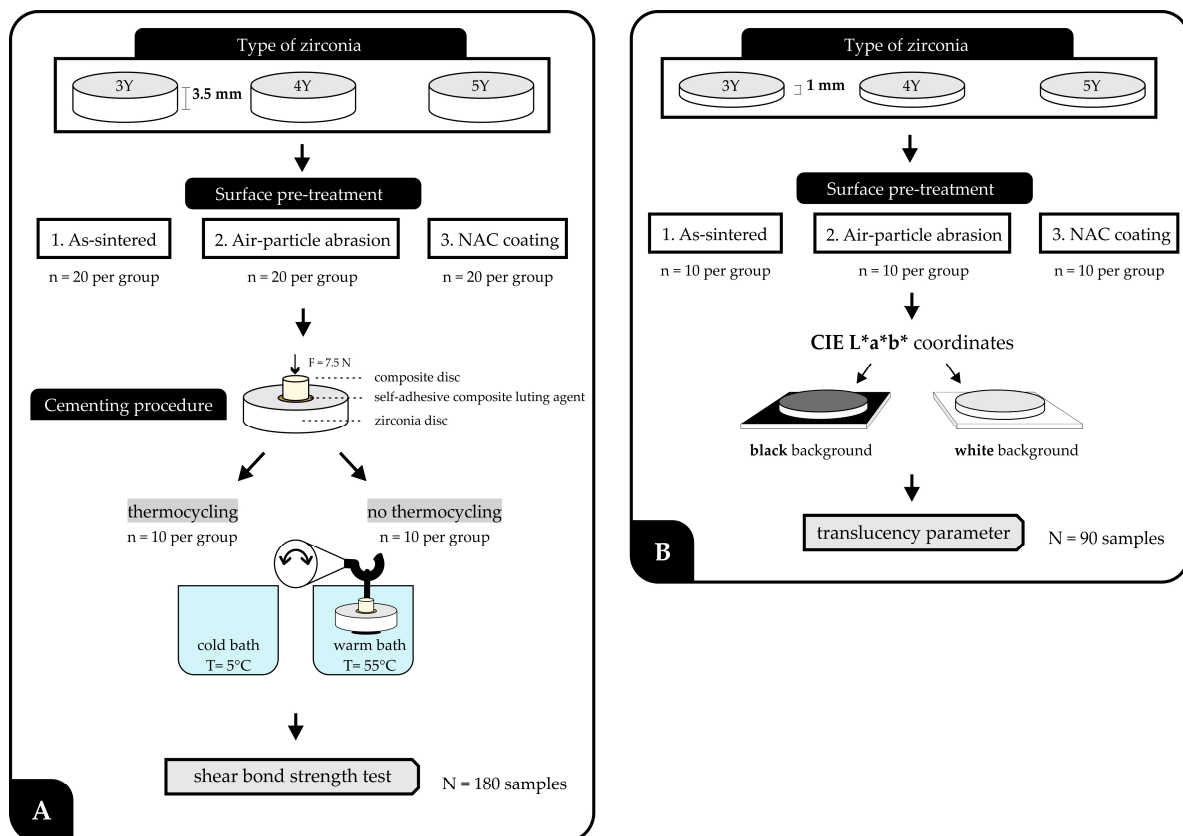


**Figure 1.** The flowchart of the experimental protocol for the (A) shear bond strength test and (B) translucency measurements.

Group 1: left as-sintered to serve as a control (AS).

Group 2: low-pressure abraded with 50-micron-sized aluminum oxide ( $\text{Al}_2\text{O}_3$ ) particles at a pressure of 0.1 MPa for 15 s (APA-50). During the air-abrasion procedure, discs were mounted in a custom-made APA device at a distance of 10 mm from the tip of the air-abrasion unit, equipped with a nozzle 0.8 mm in diameter. All the specimens were ultrasonically cleaned in acetone, ethanol, and deionized water for 3 min in each solvent.

Group 3: coated with NAC. Ten specimens were inserted into a glass beaker containing 100 mL clear, aluminate-based, precursor solution (VALLBOND, Vall-cer d.o.o., Ljubljana, Slovenia). The solution was brought to boiling in approximately 5 min using a magnetic laboratory agitator with a hot plate. The solution was boiled for 10 min until it became turbid, indicating the complete synthesis of the nanostructured boehmite coating on the specimen's surface. The coated specimens were rinsed with deionized water and oven-dried for 2 h at 110 °C (Programat X1, Ivoclar, Schaan, Lichtenstein). The calcination firing was performed in an electric resistance furnace in atmospheric air at 900 °C and a holding time of 30 min, where the heating rate was set at 40 °C/min (Programat X1, Ivoclar, Schaan, Lichtenstein) [31].

## 2.2. Shear Bond Strength Testing

### 2.2.1. Quantitative Assessment

Composite resin cylinders were fabricated by filling a printed acrylic mold with an inner diameter of 4 mm and height of 3 mm with a composite resin (TetricCeram, Ivoclar, Schaan, Liechtenstein) in two increments. Each increment was light polymerized for 20 s with a light source (Elipar II, 3M ESPE, St. Paul, MN, USA) positioned above the specimen. The composite cylinder was then removed from an acrylic mold and additionally light-cured for 20 s. Composite cylinders were bonded to Groups 1–3 using a dual-curing resin cement (Panavia V5, Kuraray, Tokyo, Japan). Before the bonding procedure, each surface

was prepared with a phosphate adhesive monomer containing primer (Ceramic Primer, Kuraray, Tokyo, Japan). A custom-made alignment apparatus was used to position the specimens to standardize the bonding procedure and ensure that the cylinder axis was perpendicular to the specimen surface. During bonding, a weight of 750 g was added to the alignment apparatus [32]. Disposable microbrushes were used to remove the excess cement, and the resin cement was polymerized for 40 s radially along the ceramic-composite cylinder interface. Glycerin gel (Oxyguard, Kuraray, Tokyo, Japan) was applied to the margins to block the oxygen inhibition layer. This is a superficial layer of resin cement exposed to oxygen, which reacts with free radicals to form unreactive peroxy radicals and inhibit polymerization [33]. Final resin cement polymerization induced by light-curing (Elipar II, 3M ESPE, St. Paul, MN, USA) was performed for 20 s.

Each surface-treated zirconia group was divided into two subgroups of ten each. The first group was stored in distilled water at 37 °C for 24 h. For investigating the durability of the resin-zirconia bond, the second group was thermally cycled (TC). TC of 37,500 cycles between 5 and 55 °C with a dwell time of 15 s (Thermocycler THE 1100, SD Mechatronik GmbH, Feldkirchen-Westerham, Germany) was utilized. Shear bond strength (SBS) was tested with a universal testing machine (Quasar 2.5, Galdabini S.P.A., Cardano Al Campo, Italy). Before testing, each specimen was mounted into a 3D printed acrylic cylinder to facilitated positioning of the specimen in the universal testing machine. A shear load was applied at the base of the specimen at a 1 mm/min crosshead speed until failure. The SBS values were expressed in MPa (N/m<sup>2</sup>).

### 2.2.2. Qualitative Assessment

Debonded zirconia surfaces for each specimen were examined using a light microscope (SteREO Discovery.V8, Carl Zeiss AG, Oberkochen, Germany) at 3.5× magnification. Failure modes were classified into adhesive failure at zirconia surface and cohesive failure in the resin cement or composite resin. The area percentage for each failure mode was calculated for all the groups in a software package (ZEN Digital Imaging for Light Microscopy, Zeiss, Oberkochen, Germany). Scanning electron microscopy (SEM; JSM-7600F, Jeol Ltd., Tokyo, Japan) at an accelerating voltage of 5 kV was used to examine debonded zirconia surfaces of the representative thermocycled specimens for each surface pretreatment. The representative specimen for each experimental group was determined as the specimen exhibiting an SBS value closest to the mean SBS value in the experimental group.

### 2.3. Translucency Measurement

For the translucency measurements, the top surfaces of the specimens were polished with silicon carbide abrasive papers (500-grit) under running water, and the thickness was verified with a digital caliper (Digimatic caliper, Mitutoyo, Kanagawa, Japan). Accepted thickness values of disc specimen were 1 ± 0.01 mm.

A dental spectrophotometer (SpectroShade™ MICRO, MHT Optic Research AG, Niederhasli, Switzerland) with a calibration plate was used to record the CIELAB coordinates ( $L^*$ ,  $a^*$  and  $b^*$ ) of the zirconia discs. The CIELAB coordinates correspond to the CIE color space defining the color data in terms of  $L^*$ ,  $a^*$  and  $b^*$ ; where  $L^*$  refers to the lightness coordinate and its value ranges from 0, for perfect black, to 100, for perfect white. The values of  $a^*$  and  $b^*$  are the coordinates in the red-green axis and the yellow-blue axis, respectively [34]. A layer of vaseline was put in-between the specimen and the background for better optical contact. Translucency was evaluated using the translucency parameter (TP) derived by calculating the color difference between reflectance spectra against a black and white background. It was reported that TP corresponds directly to the human visual perception of translucency so long as the material thickness is equal. TP was calculated according to the following equation [35]:

$$TP = \sqrt{(L_B^* - L_W^*)^2 + (a_B^* - a_W^*)^2 + (b_B^* - b_W^*)^2} \quad (1)$$

where the subscripts B and W refer to the color coordinates over black and white backgrounds, respectively, and where  $L^*$ ,  $a^*$ , and  $b^*$  refer coordinates in the CIE color space. A higher  $TP$  value indicates a higher translucency. Ten specimens were used for each condition.

#### Grain Size Estimation

Examinations of the specimen's microstructures were performed using scanning electron microscopy (SEM) of the discs' surfaces after polishing and thermal etching (SEM; Carl Zeiss AG, Oberkochen, Germany). The grain size distributions were measured on SEM micrographs according to the linear intercept method without applying any correction factor.

#### 2.4. Statistical Analysis

The statistical analysis was performed using statistical software (IBM SPSS Statistics, v20.0; IBM Corp., New York, NY, USA). Shapiro–Wilk and Levene's tests were performed to assess the assumptions of normality of the data and homogeneity of variances. For each surface pretreatment condition, independent samples  $t$ -tests were performed to assess the SBS differences between the respective non-cycled and cycled subgroups. The  $P$ -values were adjusted using the Bonferroni correction method for multiple comparisons. The SBS data were then split according to the type of zirconia and storage conditions, and a one-way ANOVA and Tukey HSD *post hoc* test were performed to assess the SBS differences for each storage condition separately. To assess the differences in the translucency between the pretreatments for each of the three types of zirconia, a one-way ANOVA with a Tukey *post hoc* test was performed.  $P$  values below 0.05 were considered statistically significant.

### 3. Results

#### 3.1. Shear Bond Strength

The alumina coating was present on the representative specimen for each type of zirconia, where NAC covered the entire as-sintered zirconia surface. In addition, 2D lamellar-like coatings' morphology was confirmed with NAC nanosheets interconnected throughout the entire zirconia surface area (Figure 2). No differences in NAC morphology were observed between the three types of zirconia.

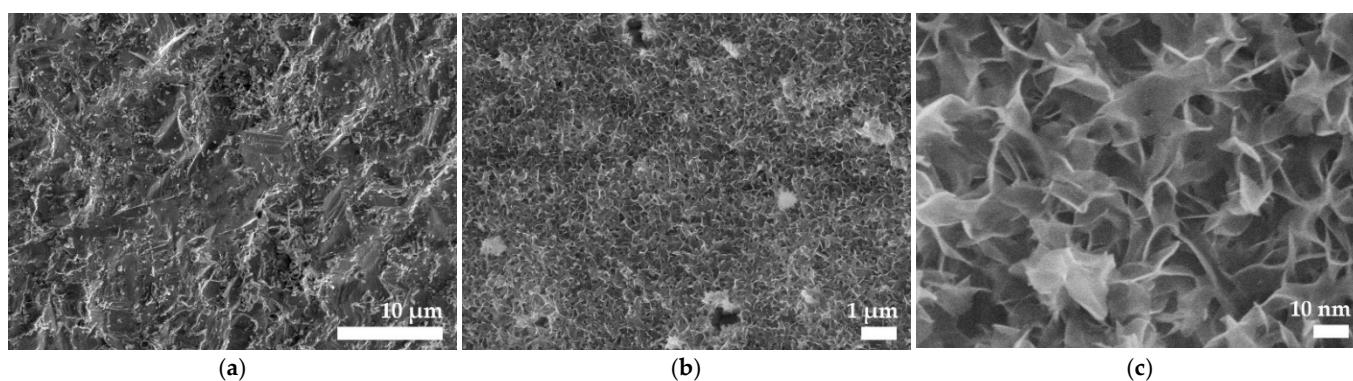


**Figure 2.** SEM micrograph showing a zirconia bonding surface that was followed by pretreatment: (a) APA resulting in surface flaws and sharp cuts (at magnification  $\times 2500$ ); (b) NAC application on the as-sintered zirconia surface (at magnification  $\times 10,000$ ); (c) NAC's lamellar-like nanostructured topography (at magnification  $\times 40,000$ ).

Means, standard deviations, and statistical differences between the SBS values of all the tested groups are shown in Table 1. Zirconia surface pretreatment and storage had a significant effect on SBS ( $P < 0.05$ ), whereas the type of zirconia ceramics did not significantly influence the SBS ( $P > 0.05$ ). In non-cycled groups, APA provided significantly higher SBS than AS, except for 3Y zirconia, where no differences between the groups were

present. NAC provided significantly higher SBS than APA, except for 3Y zirconia, where no differences between the groups were present.

**Table 1.** Shear bond strength (SBS) means and standard deviations (SD) in MPa of resin cement to the three types of zirconia ceramics after different surface pretreatment methods. Same upper-case letters denote no statistical differences in SBS values among the groups ( $P < 0.05$ ).

Type of ZrO <sub>2</sub>	Treatment	No Thermocycling			37,500 Thermocycles		
		Mean	SD	<i>P</i> < 0.05	Mean	SD	<i>P</i> < 0.05
3Y	AS	11.88	2.44	A	0.00	ds	A
	APA	18.16	2.24	C, D, E	14.25	4.00	B
	NAC	22.19	5.82	E, F	21.52	2.63	C
4Y	AS	14.00	3.11	A, B, C	0.00	ds	A
	APA	17.30	2.59	B, C, D	15.27	4.05	B
	NAC	23.43	1.52	F	20.10	4.63	C
5Y	AS	12.93	2.72	A, B	0.00	ds	A
	APA	15.81	4.16	A, B, C	12.17	2.21	B
	NAC	21.57	2.46	D, E, F	23.06	3.74	C

ds—debonded spontaneously, no statistical test was performed.

After TC, AS groups exhibited spontaneous debonding in a complete adhesive failure. Although lowered SBS was observed, TC did not significantly affect NAC and APA groups. NAC provided significantly higher SBS than APA for all three types of zirconia.

The area percentages of cohesive and adhesive failure mode after SBS testing are presented in Figure 3. For the AS groups, mixed failure modes with a high percentage of adhesive failure were observed. In contrast, mixed failure mode with a high percentage of cohesive failure was observed in APA and NAC groups. In addition, complete cohesive failure mode, although in a smaller portion, was also observed in the APA and NAC groups. After TC, the percentage of adhesive failure area slightly lowered in all the groups.

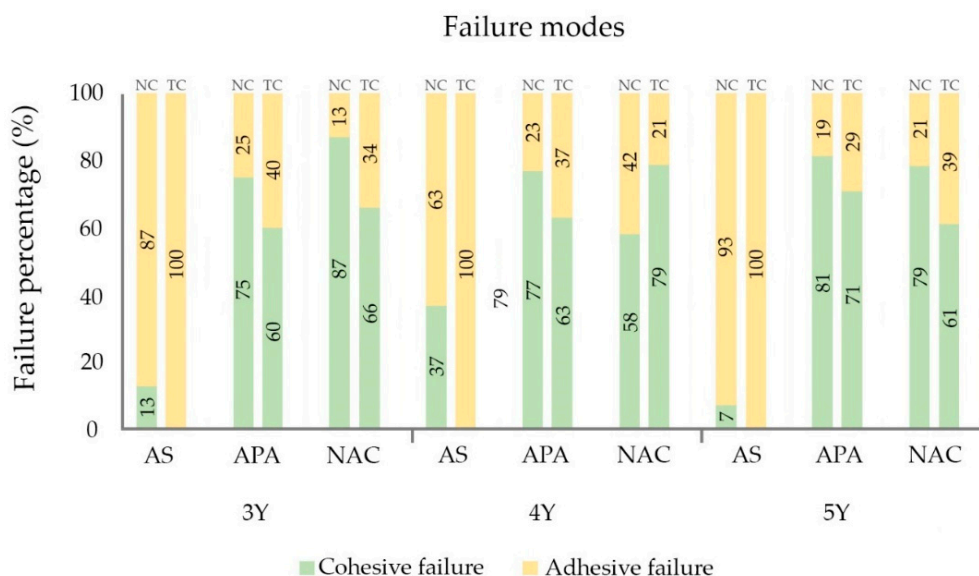


**Figure 3.** Mean percentages of assigned failure modes after shear bond testing of non-cycled (NC) and cycled (TC) groups.

Light microscopy micrographs and SEM micrographs of representative specimens for AS, APA, and NAC groups after SBS testing are presented in Figure 4a–c. In the representative AS specimen, complete adhesive failure was observed (Figure 4a), while mixed failure mode with a high percentage of cohesive failure was observed in the representative APA

specimen (Figure 4b). In the representative NAC specimen, mainly cohesive failure mode was observed, with the composite resin or resin cement fracture (Figure 4c). NAC residues were partially covered with cement remnants and remained firmly bonded to the substrate after the fracture (Figure 4c).

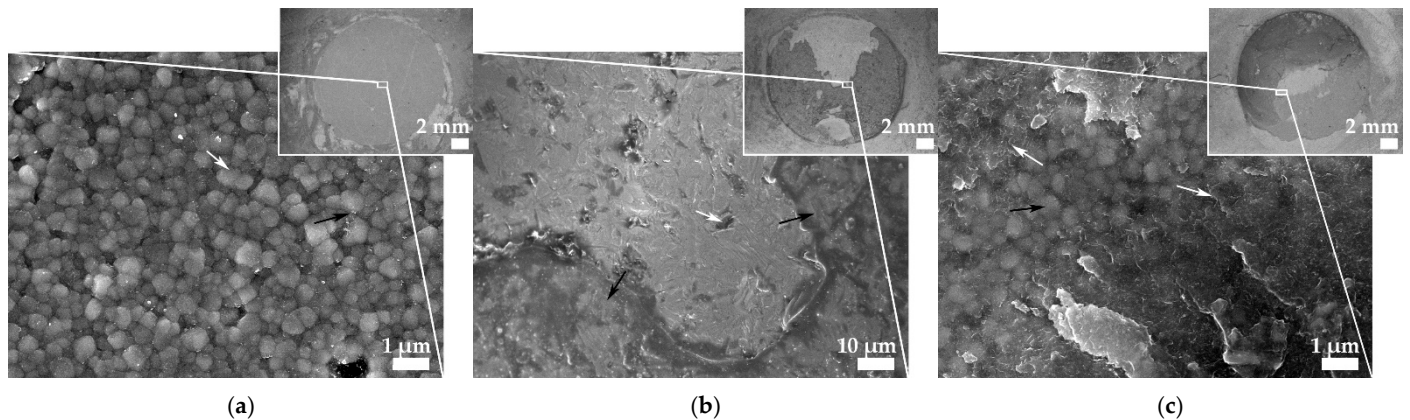


**Figure 4.** Light microscopy micrographs (insets) and SEM micrographs of different failure modes of representative specimens: (a) adhesive failure mode of AS specimen—at magnification  $\times 3.5$  complete adhesive failure is evident and at magnification  $\times 10,000$  exposed zirconia grains (white arrow) and residing cement fillers (black arrow) are observed; (b) mixed failure mode of APA specimen - at magnification  $\times 3.5$  a low percentage of adhesive failure is evident and, at magnification  $\times 1000$ , cement remnants (black arrow), surface flaws, and sharp indentations (white arrows) caused by APA are observed; (c) mixed failure mode with a predominantly cohesive fracture of an NAC specimen, at magnification  $\times 3.5$  thick cement residue (white arrow), is observed with a small adhesive failure and, at magnification  $\times 10,000$ , exposed zirconia grains covered with NAC residue (white arrows) are observed.

### 3.2. Translucency

SEM micrographs of polished and thermally etched 3Y, 4Y, and 5Y zirconia are shown in Figure 5a–f. The microstructure of the zirconia ceramics revealed polycrystalline and dense structures with only occasionally very few pores. The three zirconia ceramics differed in microstructure for grain size. The size of the zirconia grains increased with the amount of yttria; the largest grains were observed in the 5Y group. The  $d_{50}$  diameters of 3Y, 4Y, and 5Y were 0.28, 0.32, and 0.53  $\mu\text{m}$ , respectively.

The translucency parameter (TP) significantly differed between different types of zirconia ceramics (ANOVA, Tukey  $P < 0.05$ ); the lowest TP was observed in the 3Y-APA group (21.4) and the highest in the 5Y-AS group (31.9) (see Table 2 and Figure 6). From Figure 6, the difference in translucency can be qualitatively observed by the level of sharpness seen in the thick black line onto which the specimens were placed. APA significantly decreased the TP of all three types of zirconia ceramics. In contrast, nanostructured alumina coating did not interfere with TP changes (Table 2). The observed mean differences of TP are presented in Table 3.

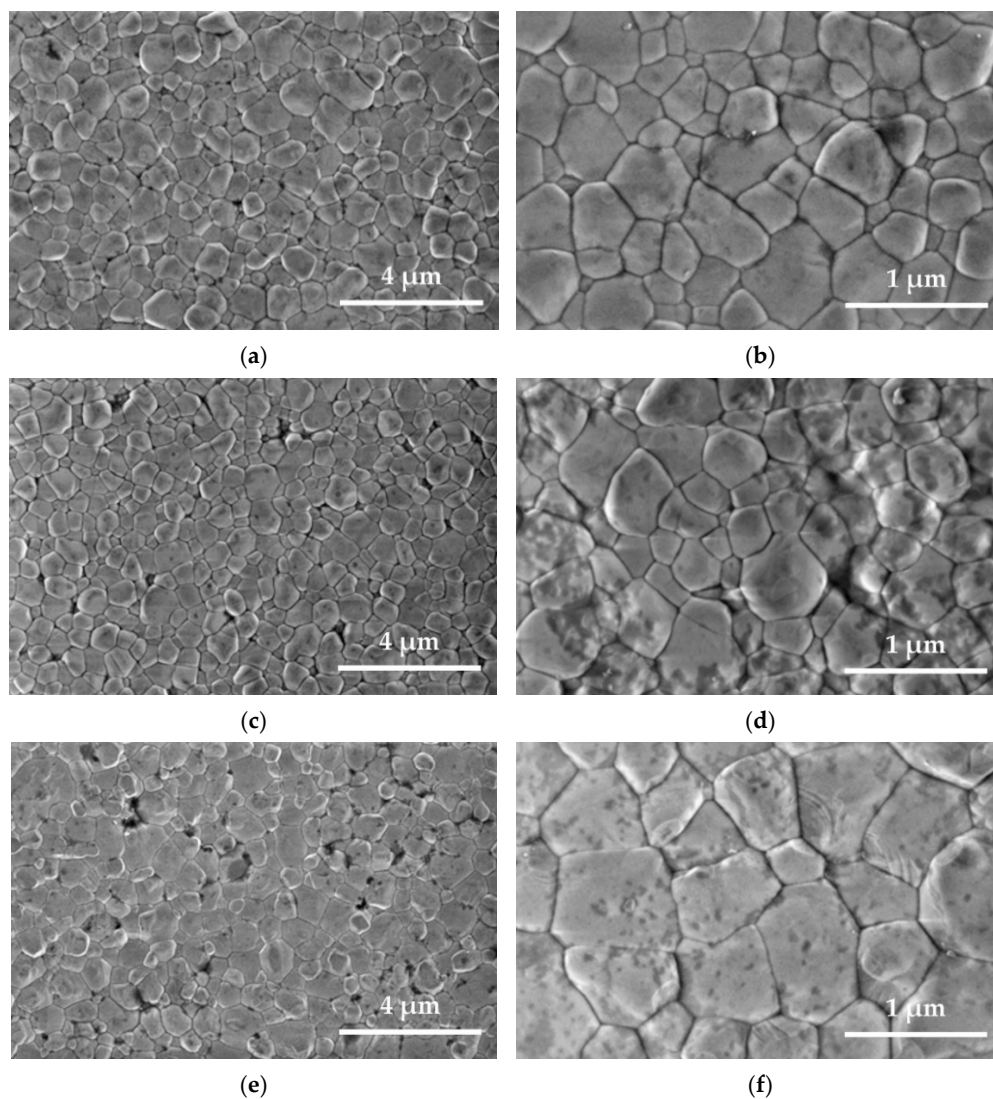


**Figure 5.** SEM micrographs of as-sintered zirconia surface at magnification  $\times 25,000$  (left) and magnification  $\times 60,000$  (right): 3Y specimen (a,b), 4Y specimen (c,d), and 5Y specimen (e,f).

**Table 2.** Translucency parameter means (Mean TP) and standard deviations (SD) of different types of zirconia ceramics treated with APA and NAC. The same upper-case letters denote no statistical differences in TP values among the groups ( $P < 0.05$ ).

Type of ZrO <sub>2</sub>	Treatment	Mean TP	SD	$P < 0.05$
3Y	AS	23.4	0.64	A
	NAC	23.6	0.21	A
	APA	21.4	0.13	B
4Y	AS	25.7	0.39	C
	NAC	25.6	0.56	C
	APA	24.4	0.18	D
5Y	AS	31.9	1.05	E
	NAC	31.8	0.54	E
	APA	29.9	0.76	F

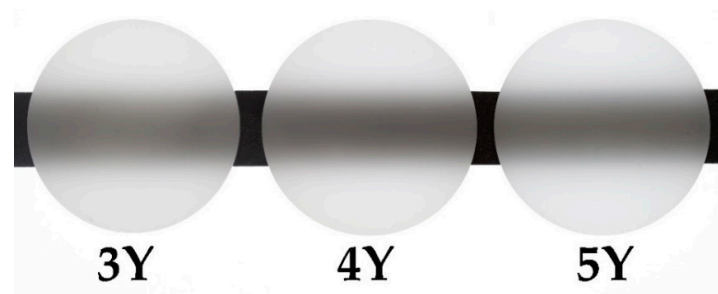


**Figure 6.** The translucency of zirconia ceramics (3Y, 4Y, 5Y) in 1 mm thickness.

**Table 3.**  $\Delta TP_{ab}$ —observed mean differences of TP between different types of surface treatment. Letter *P* denotes the level of significance (*P*-value).

$\Delta TP_{ab}$	3Y				4Y				5Y			
	NAC	<i>P</i>	APA	<i>P</i>	NAC	<i>P</i>	APA	<i>P</i>	NAC	<i>P</i>	APA	<i>P</i>
AS	−0.26	0.55	1.92	<0.001	0.07	0.96	1.24	0.001	0.19	0.93	2.05	0.005
NAC	-	-	2.18	<0.001	-	-	1.16	0.002	-	-	1.86	0.009

#### 4. Discussion

This study has shown that NAC provided higher resin-zirconia bond strengths compared to APA, not affecting the zirconia optical properties. APA, on the other hand, lowered the translucency of all types of zirconia. Therefore, the null hypotheses were rejected.

The 3Y zirconia studied, also known as high-translucent 3Y-TZP, contains less alumina in the matrix than conventional 3Y-TZP, thus hindering the formation of isolated, light obstructing alumina grains at the grain boundaries [36,37]. In the 4Y and 5Y zirconia, yttria content is increased to 4 and 5 mol.%, respectively, leading to a higher amount of larger, and less birefringent, cubic grains; lowering incident light scattering [37]. The measured differences in grain sizes for three types of zirconia and calculated TPs corroborate these findings (Table 2). TP increased with the grain size of 3Y to 5Y zirconia, consistent with correlations reported in previous studies [38]. Furthermore, the optical properties of 5Y zirconia are comparable to other translucent non-oxide dental ceramics while maintaining superior mechanical properties [39]. Therefore, its application can be extended to the fabrication of thin esthetic monolithic zirconia restorations.

Debonding of such non-retentive zirconia restorations remains the main clinical complication [7]. Among the few studies that evaluated the bond strength to newer translucent zirconia [39–42], some have reported lower bond strength than conventional 3Y-TZP [40]. In the present study, APA; a surface damaging pretreatment method, introduced surface, and subsurface, cracks into the material. By contrast, NAC; a nondamaging pretreatment method, only additively modified the surface by increasing the surface's roughness, whereas the AS group served as a control. TC of 37,500 cycles were utilized for the purpose of investigating the durability of resin-zirconia bonds generating mechanical fatigue at the bonding interface [41,42].

Despite lower SBS values after 24 h of water storage in the AS groups, there were no statistically significant differences detected between the AS and APA groups, except with respect to the 3Y material (Table 1). The relatively high initial bond strength was probably provided by the chemical bonding provided by 10-methacryloyloxydecyl dihydrogen phosphate (MDP) adhesive monomer containing primer, which was previously reported as highly efficient [18,43,44]. After TC, the AS specimens debonded spontaneously (Table 1), confirming the inability of phosphate adhesive monomer to create hydrolytically stable chemical bonds to zirconia without any mechanical interlocking [6,18]. Therefore, micro-mechanical roughening with APA in combination with adhesive monomer remains the proposed pretreatment for the translucent zirconia [43,45,46]. APA, under low air-abrasion

pressure of 0.1 MPa, was employed in the present study since it provides a stable resin bond to conventional zirconia while reducing the damaging surface effects [18].

The SBS values in APA groups for all three types of zirconia were not affected by TC (Table 1). These findings confirm that the increased surface roughness and wettability provided by APA present a prerequisite for hydrolysis-resistant chemical bonding to zirconia [18,44]. However, these results are not completely in line with previous studies [18,44] where, even after TC, a resin-zirconia bond above 20 MPa was achieved, demonstrating a clinically acceptable, and durable, bond to enamel [47,48]. While increasing air-abrasion pressure to 0.2 MPa provides an optimal bonding surface topography for a durable bond to translucent zirconia [45,46], these more aggressive APA conditions are reported to decrease the flexural strength of translucent zirconia [49]. The differences in SBS values between different types of zirconia pretreated with APA were undetected. Although the surface roughness of 5Y zirconia after APA had previously been shown to be slightly higher [45], no impact on the bond strength was detected, confirming the results of our study. Since, during TC, the specimens were exposed to moist conditions only for a short time period, no low thermal degradation (LTD) of zirconia, which could lead to the material microstructure changes, could be expected [50]. Moreover, 4Y and 5Y zirconia materials were shown to be resistant towards LTD [51]. In light of this evidence, no other influence of TC on the zirconia microstructure and resin-zirconia interface aside from the mechanical fatigue at the bonding interface, could be expected. Therefore, the influence of a zirconia chemical composition might not have been assessed using the aging protocol. A previously measured, 500–700 nm, layer of NAC [26], with its lamellar-like topography, provides an increase of the actual surface area up to 500%–600% [52]. This has also been shown using transmission electron microscopy (TEM) where the resin cement successfully penetrates into the nano-dimensional inter-lamellar spaces, forming an intermediate structure designated as the hybrid layer [31]. No voids or signs of delamination were observed in the SEM micrographs (Figure 2), indicating the coating being coherently adhered on the zirconia surface, which is in line with the previous TEM analyses [26,31]. Therefore, the NAC-modified surface significantly enhanced resin-zirconia SBS values for all three types of zirconia (Table 1 and Figure 3). These findings are in line with NAC's superior *in vitro* performance on bonding to conventional zirconia [26,27]. In addition, only in NAC groups did SBS values reach a clinically adequate SBS value of 20 MPa [47,48] even after TC, which did not affect the bond durability. SBS values for different pretreatment methods corroborated well with the evaluated failure modes (Figures 3 and 4). An adhesive type was observed for the AS groups, whereas the predominantly mixed type was observed for APA and NAC groups with a lower percentage of adhesive fracture slightly increasing after TC, was observed. These observations indicate stable bonds to zirconia provided by both pretreatments. Furthermore, SEM analysis of a representative NAC specimen revealed only small areas of exposed zirconia grains. In contrast, large areas of exposed NAC residues, or NAC covered with resin cement, were observed, indicating that NAC did not delaminate from the zirconia surface. As shown previously, this may suggest the formation of strong bonds between NAC and zirconia [26,27,31].

The irregularities at the zirconia surface introduced by APA increases the diffuse reflectance of the incident light, which affects zirconia's optical properties. The present results are in line with these findings since APA significantly decreased TP regardless of the type of zirconia (Table 2). The surface roughness provided by APA increases diffuse reflectance and affects the specular reflectance, thereby contributing to the lower levels of translucency [53]. Furthermore, compared to the micro-irregularities produced by APA, NAC exhibits nano-particles in the size of a few nm (Figure 2b), which is considerably smaller than the incident wavelength of visible light (400–700 nm) and, therefore, could minimize diffuse reflectance [54,55]. Unchanged TP in the NAC groups (Table 2) suggest that NAC reduced diffuse reflectance while not affecting the zirconia optical properties. Furthermore, the obtained mean APA-NAC differences in TP for the 3Y and 5Y zirconia

(Table 3) are clinically relevant since the translucency perceptibility threshold (1.33) [56] was exceeded.

While NAC facilitates adhesive dentistry, frequently without the need for tooth preparation, a high risk of saliva, blood, and aerosol contamination during drilling procedures can be avoided [57,58]. In addition, minor preparations needed for non-retentive zirconia restorations treated with NAC might contribute to treating patients with specific disorders, such as saliva deficiency and reduced enamel quality, where reduction of dental tissues for retentive reasons may be detrimental to the long-term rehabilitation success [59]. Moreover, it has been shown that NAC's nano-morphology induces osteoblast differentiation while concurrently inhibiting bacterial adhesion [60]. These phenomena may be implemented in zirconia implant surface modifications or other bone regenerative procedures [61–63].

Limitations of the present study include a simplified experimental model not involving natural teeth and the use of a high-stress concentrating SBS test. This study investigated the resin-zirconia bond since NAC affects only the resin-zirconia interface. Moreover, failure of this interface is a frequent complication of non-retentive zirconia restorations, thus, our experimental model did not include natural teeth, excluding the unproblematic enamel-resin interface [30,64]. The SBS test used here is widely used to evaluate bond strength because of its simplicity. However, this test develops high-stress concentrations in the adhesive interface. Therefore, a bond strength test inducing more stable crack propagation may be beneficial to further explore the NAC's bonding capacity [65,66].

## 5. Conclusions

Based on the findings of this *in vitro* study, the following conclusions were drawn:

1. NAC provided significantly higher SBS of resin cement to all types of translucent zirconia than APA.
2. NAC did not affect the optical properties, while APA significantly lowered the translucency of translucent zirconia.
3. NAC, not impairing mechanical nor optical properties of translucent zirconia, should be regarded as a zirconia pretreatment alternative to APA.

**Author Contributions:** The first two authors T.M. (Tine Malgaj) and T.M. (Tadej Mirt) contributed equally to the work. Conceptualization, T.M. (Tine Malgaj), T.M. (Tadej Mirt), A.K. and P.J.; Methodology, T.M. (Tine Malgaj), T.M. (Tadej Mirt) and A.K.; Investigation, T.M. (Tine Malgaj), T.M. (Tadej Mirt) and A.K.; Writing—original draft preparation, T.M. (Tine Malgaj) and T.M. (Tadej Mirt); Writing—review and editing, A.K.; Formal analysis, T.M. (Tine Malgaj) and T.M. (Tadej Mirt); Supervision, P.J. and A.K.; Funding Acquisition, A.K. and P.J.; Project Administration, P.J.; Validation, A.K. and P.J.; Visualization, T.M. (Tine Malgaj), T.M. (Tadej Mirt) and A.K. All authors have read and agreed to the published version of the manuscript.

**Funding:** This work was supported by the Slovenian Research Agency funding through research project towards reliable implementation of monolithic zirconia dental restorations (J2-9222) and research program Ceramics and complementary materials for advanced engineering and biomedical applications (P2-0087).

**Institutional Review Board Statement:** Not applicable.

**Informed Consent Statement:** Not applicable.

**Data Availability Statement:** Not applicable.

**Acknowledgments:** The authors thank Jitka Hreščak for conducting the SEM examination of the specimen microstructure.

**Conflicts of Interest:** The authors declare no conflict of interest.

## References

1. Manicone, P.F.; Rossi Iommetti, P.; Raffaelli, L. An overview of zirconia ceramics: Basic properties and clinical applications. *J. Dent.* **2007**, *35*, 819–826. [[CrossRef](#)]
2. Della Bona, A.; Kelly, J.R. The clinical success of all-ceramic restorations. *J. Am. Dent. Assoc.* **2008**, *139*, 8S–13S. [[CrossRef](#)]

3. Al-Amleh, B.; Lyons, K.; Swain, M. Clinical trials in zirconia: A systematic review. *J. Oral Rehabil.* **2010**, *37*, 641–652. [[CrossRef](#)]
4. Denry, I.; Kelly, J.R. State of the art of zirconia for dental applications. *Dent. Mater.* **2008**, *24*, 299–307. [[CrossRef](#)] [[PubMed](#)]
5. Zhang, Y.; Lawn, B.R. Novel zirconia materials in dentistry. *J. Dent. Res.* **2018**, *97*, 140–147. [[CrossRef](#)] [[PubMed](#)]
6. Ozcan, M.; Bernasconi, M. Adhesion to zirconia used for dental restorations: A systematic review and meta-analysis. *J. Adhes. Dent.* **2015**, *17*, 7–26. [[PubMed](#)]
7. Chen, J.; Cai, H.; Ren, X.; Suo, L.; Pei, X.; Wan, Q. A Systematic review of the survival and complication rates of all-ceramic resin-bonded fixed dental prostheses. *J. Prosthodont.* **2018**, *27*, 535–543. [[CrossRef](#)] [[PubMed](#)]
8. Quigley, N.P.; Loo, D.S.S.; Choy, C.; Ha, W.N. Clinical efficacy of methods for bonding to zirconia: A systematic review. *J. Prosthet. Dent.* **2021**, *125*, 231–240. [[CrossRef](#)] [[PubMed](#)]
9. Atsu, S.S.; Kilicarslan, M.A.; Kucukesmen, H.C.; Aka, P.S. Effect of zirconium-oxide ceramic surface treatments on the bond strength to adhesive resin. *J. Prosthet. Dent.* **2006**, *95*, 430–436. [[CrossRef](#)]
10. Derand, T.; Molin, M.; Kvam, K. Bond strength of composite luting cement to zirconia ceramic surfaces. *Dent. Mater.* **2005**, *21*, 1158–1162. [[CrossRef](#)]
11. Lung, C.Y.; Kukk, E.; Matinlinna, J.P. The effect of silica-coating by sol-gel process on resin-zirconia bonding. *Dent. Mater. J.* **2013**, *32*, 165–172. [[CrossRef](#)] [[PubMed](#)]
12. Everson, P.; Addison, O.; Palin, W.M.; Burke, F.J. Improved bonding of zirconia substructures to resin using a “glaze-on” technique. *J. Dent.* **2012**, *40*, 347–351. [[CrossRef](#)]
13. Phark, J.H.; Duarte, S., Jr.; Blatz, M.; Sadan, A. An in vitro evaluation of the long-term resin bond to a new densely sintered high-purity zirconium-oxide ceramic surface. *J. Prosthet. Dent.* **2009**, *101*, 29–38. [[CrossRef](#)]
14. Egilmez, F.; Ergun, G.; Cekic-Nagas, I.; Vallittu, P.K.; Ozcan, M.; Lassila, L.V. Effect of surface modification on the bond strength between zirconia and resin cement. *J. Prosthodont.* **2013**, *22*, 529–536. [[CrossRef](#)]
15. Aboushelib, M.N.; Kleverlaan, C.J.; Feilzer, A.J. Selective infiltration-etching technique for a strong and durable bond of resin cements to zirconia-based materials. *J. Prosthet. Dent.* **2007**, *98*, 379–388. [[CrossRef](#)]
16. Yang, X.; Liu, Y. Influence of different surface treatments on zirconia/resin shear bond strength using one-bottle universal adhesive. *Adv. Appl. Ceram.* **2018**, *118*, 70–77. [[CrossRef](#)]
17. Wolfart, M.; Lehmann, F.; Wolfart, S.; Kern, M. Durability of the resin bond strength to zirconia ceramic after using different surface conditioning methods. *Dent. Mater.* **2007**, *23*, 45–50. [[CrossRef](#)] [[PubMed](#)]
18. Yang, B.; Barloi, A.; Kern, M. Influence of air-abrasion on zirconia ceramic bonding using an adhesive composite resin. *Dent. Mater.* **2010**, *26*, 44–50. [[CrossRef](#)] [[PubMed](#)]
19. Zhang, Y.; Lawn, B.R.; Rekow, E.D.; Thompson, V.P. Effect of sandblasting on the long-term performance of dental ceramics. *J. Biomed. Mater. Res. B Appl. Biomater.* **2004**, *71*, 381–386. [[CrossRef](#)]
20. Zhang, Y.; Lawn, B.R.; Malament, K.A.; Van Thompson, P.; Rekow, E.D. Damage accumulation and fatigue life of particle-abraded ceramics. *Int. J. Prosthodont.* **2006**, *19*, 442–448.
21. Wang, H.; Aboushelib, M.N.; Feilzer, A.J. Strength influencing variables on CAD/CAM zirconia frameworks. *Dent. Mater.* **2008**, *24*, 633–638. [[CrossRef](#)] [[PubMed](#)]
22. Oblak, C.; Verdenik, I.; Swain, M.V.; Kosmac, T. Survival-rate analysis of surface treated dental zirconia (Y-TZP) ceramics. *J. Mater. Sci. Mater. Med.* **2014**, *25*, 2255–2264. [[CrossRef](#)]
23. Oblak, C.; Kocjan, A.; Jevnikar, P.; Kosmač, T. The effect of mechanical fatigue and accelerated ageing on fracture resistance of glazed monolithic zirconia dental bridges. *J. Eur. Ceram. Soc.* **2017**, *37*, 4415–4422. [[CrossRef](#)]
24. Guth, J.F.; Stawarczyk, B.; Edelhoff, D.; Liebermann, A. Zirconia and its novel compositions: What do clinicians need to know? *Quintessence Int.* **2019**, *50*, 512–520. [[PubMed](#)]
25. Lawson, N.C.; Jurado, C.A.; Huang, C.T.; Morris, G.P.; Burgess, J.O.; Liu, P.R.; Kinderknecht, K.E.; Lin, C.P.; Givan, D.A. Effect of Surface Treatment and Cement on Fracture Load of Traditional Zirconia (3Y), Translucent Zirconia (5Y), and Lithium Disilicate Crowns. *J. Prosthodont.* **2019**, *28*, 659–665. [[CrossRef](#)]
26. Malgaj, T.; Kocjan, A.; Jevnikar, P. The effect of firing protocols on the resin-bond strength to alumina-coated zirconia ceramics. *Adv. Appl. Ceram.* **2019**, *119*, 267–275. [[CrossRef](#)]
27. Jevnikar, P.; Golobič, M.; Kocjan, A.; Kosmač, T. The effect of nano-structured alumina coating on the bond strength of resin-modified glass ionomer cements to zirconia ceramics. *J. Eur. Ceram. Soc.* **2012**, *32*, 2641–2645. [[CrossRef](#)]
28. Kocjan, A. The hydrolysis of AlN powder—a powerful tool in advanced materials engineering. *Chem. Rec.* **2018**, *18*, 1–16. [[CrossRef](#)] [[PubMed](#)]
29. Malgaj, T.; Plut, A.; Eberlinc, A.; Drevensek, M.; Jevnikar, P. Anterior esthetic rehabilitation of an alveolar cleft using novel minimally invasive prosthodontic techniques: A case report. *Cleft Palate Craniofac. J.* **2021**, *58*, 912–918. [[CrossRef](#)] [[PubMed](#)]
30. Malgaj, T.; Abram, A.; Kocjan, A.; Jevnikar, P. Influence of nanostructured alumina coating on the clinical performance of zirconia cantilevered resin-bonded fixed dental prostheses: Up to 3-year results of a prospective, randomized, controlled clinical trial. *J. Prosthet. Dent.* **2021**, in press. [[CrossRef](#)]
31. Jevnikar, P.; Krnel, K.; Kocjan, A.; Funduk, N.; Kosmac, T. The effect of nano-structured alumina coating on resin-bond strength to zirconia ceramics. *Dent. Mater.* **2010**, *26*, 688–696. [[CrossRef](#)] [[PubMed](#)]
32. Hummel, M.; Kern, M. Durability of the resin bond strength to the alumina ceramic Procera. *Dent. Mater.* **2004**, *20*, 498–508. [[CrossRef](#)]

33. Finger, W.J.; Lee, K.S.; Podszun, W. Monomers with low oxygen inhibition as enamel/dentin adhesives. *Dent. Mater.* **1996**, *12*, 256–261. [[CrossRef](#)]
34. Commission Internationale de l'Éclairage. *CIE Technical Report: Colorimetry*; CIE Publication: Paris, France, 2004.
35. Della Bona, A.; Nogueira, A.D.; Pecho, O.E. Optical properties of CAD-CAM ceramic systems. *J. Dent.* **2014**, *42*, 1202–1209. [[CrossRef](#)]
36. Klimke, J.; Trunec, M.; Krell, A. Transparent tetragonal yttria-stabilized zirconia ceramics: Influence of scattering caused by birefringence. *J. Am. Ceram. Soc.* **2011**, *94*, 1850–1858. [[CrossRef](#)]
37. Krell, A.; Hutzler, T.; Klimke, J. Transmission physics and consequences for materials selection, manufacturing, and applications. *J. Eur. Ceram. Soc.* **2009**, *29*, 207–221. [[CrossRef](#)]
38. Fathy, S.M.; Al-Zordk, W.; Grawish, M.E.; Swain, M.V. Flexural strength and translucency characterization of aesthetic monolithic zirconia and relevance to clinical indications: A systematic review. *Dent. Mater.* **2021**, *37*, 711–730. [[CrossRef](#)]
39. Zhang, F.; Reveron, H.; Spies, B.C.A. Trade-off between fracture resistance and translucency of zirconia and lithium-disilicate glass ceramics for monolithic restorations. *Acta Biomater.* **2019**, *91*, 24–34. [[CrossRef](#)]
40. Ruales-Carrera, E.; Cesar, P.F.; Henriques, B.; Fredel, M.C.; Ozcan, M.; Volpato, C.A.M. Adhesion behavior of conventional and high-translucent zirconia: Effect of surface conditioning methods and aging using an experimental methodology. *J. Esthet. Restor. Dent.* **2019**, *31*, 388–397. [[CrossRef](#)]
41. Heikkinen, T.T.; Matinlinna, J.P.; Vallittu, P.K.; Lassila, L.V. Long term water storage deteriorates bonding of composite resin to alumina and zirconia short communication. *Open Dent. J.* **2013**, *7*, 123–125. [[CrossRef](#)]
42. Gale, M.S.; Darvell, B.W. Thermal cycling procedures for laboratory testing of dental restorations. *J. Dent.* **1999**, *27*, 89–99. [[CrossRef](#)]
43. Valente, F.; Mavriqi, L.; Traini, T. Effects of 10-MDP based primer on shear bond strength between zirconia and new experimental resin cement. *Materials* **2020**, *13*, 235. [[CrossRef](#)]
44. Kern, M.; Barloi, A.; Yang, B. Surface conditioning influences zirconia ceramic bonding. *J. Dent. Res.* **2009**, *88*, 817–822. [[CrossRef](#)] [[PubMed](#)]
45. Aung, S.; Takagaki, T.; Lyann, S.K.; Ikeda, M.; Inokoshi, M.; Sadr, A.; Nikaido, T.; Tagami, J. Effects of alumina-blasting pressure on the bonding to super/ultra-translucent zirconia. *Dent. Mater.* **2019**, *35*, 730–739. [[CrossRef](#)]
46. Zhang, X.; Liang, W.; Jiang, F.; Wang, Z.; Zhao, J.; Zhou, C.; Wu, J. Effects of air-abrasion pressure on mechanical and bonding properties of translucent zirconia. *Clin. Oral Investig.* **2021**, *25*, 1979–1988. [[CrossRef](#)]
47. Papia, E.; Larsson, C.; du Toit, M.; Vult von Steyern, P. Bonding between oxide ceramics and adhesive cement systems: A systematic review. *J. Biomed. Mater. Res. B Appl. Biomater.* **2014**, *102*, 395–413. [[CrossRef](#)] [[PubMed](#)]
48. Van Meerbeek, B.; Peumans, M.; Poitevin, A.; Mine, A.; Van Ende, A.; Neves, A.; De Munck, J. Relationship between bond-strength tests and clinical outcomes. *Dent. Mater.* **2010**, *26*, e100–e121. [[CrossRef](#)]
49. Yoshida, K. Influence of alumina air-abrasion for highly translucent partially stabilized zirconia on flexural strength, surface properties, and bond strength of resin cement. *J. Appl. Oral Sci.* **2020**, *28*, e20190371. [[CrossRef](#)] [[PubMed](#)]
50. Keuper, M.; Berthold, C.; Nickel, K.G. Long-time aging in 3 mol.% yttria-stabilized tetragonal zirconia polycrystals at human body temperature. *Acta Biomater.* **2014**, *10*, 951–959. [[CrossRef](#)] [[PubMed](#)]
51. Camposilvan, E.; Leone, R.; Gremillard, L.; Sorrentino, R.; Zarone, F.; Ferrari, M.; Chevalier, J. Aging resistance, mechanical properties and translucency of different yttria-stabilized zirconia ceramics for monolithic dental crown applications. *Dent. Mater.* **2018**, *34*, 879–890. [[CrossRef](#)] [[PubMed](#)]
52. Kocjan, A.; Ambrožič, M.; Kosmač, T. Stereometric analysis of nanostructured boehmite coatings synthesized by aluminum nitride powder hydrolysis. *Ceram. Int.* **2012**, *38*, 4853–4859. [[CrossRef](#)]
53. Liu, G.L.; Huang, Z.R.; Liu, X.J.; Jiang, D.L. Effect of density and surface roughness on optical properties of silicon carbide optical components. *Chin. Phys. Lett.* **2008**, *25*, 1135–1137.
54. Guinneton, F.; Valmalette, J.C.; Gavarri, J.R. Nanocrystalline vanadium dioxide: Synthesis and mid-infrared properties. *Opt. Mater.* **2000**, *15*, 111–114. [[CrossRef](#)]
55. Guinneton, F.; Sauques, L.; Valmalette, J.C.; Cros, F.; Gavarri, J.R. Role of surface defects and microstructure in infrared optical properties of thermochromic VO<sub>2</sub> materials. *J. Phys. Chem. Solids* **2005**, *66*, 63–73. [[CrossRef](#)]
56. Salas, M.; Lucena, C.; Herrera, L.J.; Yebra, A. Translucency thresholds for dental materials. *Dent. Mater.* **2018**, *34*, 1168–1174. [[CrossRef](#)]
57. Gherlone, E.; Polizzi, E.; Tete, G.; Cappare, P. Dentistry and Covid-19 pandemic: Operative indications post-lockdown. *New Microbiol.* **2021**, *44*, 1–11. [[PubMed](#)]
58. Tecco, S.; Parisi, M.R.; Gastaldi, G.; Polizzi, E.; D'Amicantonio, T.; Zilocchi, I.; Gardini, I.; Gherlone, E.F.; Lazzarin, A.; Cappare, P. Point-of-care testing for hepatitis C virus infection at an Italian dental clinic: Portrait of the pilot study population. *New Microbiol.* **2019**, *42*, 133–138. [[PubMed](#)]
59. D'Orto, B.; Tete, G.; Polizzi, E. Osseointegrated dental implants supporting fixed prostheses in patients affected by Sjogren's Syndrome: A narrative review. *J. Biol. Regul. Homeost. Agents* **2020**, *34*, 91–93. [[PubMed](#)]
60. Moritz, J.; Abram, A.; Čekada, M.; Gabor, U.; Garvas, M.; Zdovc, I.; Dakskobler, A.; Cotič, J.; Ivičak-Kocjan, K.; Kocjan, A. Nanoroughening of sandblasted 3Y-TZP surface by alumina coating deposition for improved osseointegration and bacteria reduction. *J. Eur. Ceram. Soc.* **2019**, *39*, 4347–4357. [[CrossRef](#)]

61. Tete, G.; D'Orto, B.; Nagni, M.; Agostinacchio, M.; Polizzi, E.; Agliardi, E. Role of induced pluripotent stem cells (IPSCS) in bone tissue regeneration in dentistry: A narrative review. *J. Biol. Regul. Homeost. Agents* **2020**, *34*, 1–10.
62. Cappare, P.; Tete, G.; Sberna, M.T.; Panina-Bordignon, P. The emerging role of stem cells in regenerative dentistry. *Curr. Gene Ther.* **2020**, *20*, 259–268. [[CrossRef](#)] [[PubMed](#)]
63. Crespi, R.; Cappare, P.; Gherlone, E. Sinus floor elevation by osteotome: Hand mallet versus electric mallet. A prospective clinical study. *Int. J. Oral Maxillofac. Implants* **2012**, *27*, 1144–1150.
64. Sterzenbach, G.; Tunjan, R.; Rosentritt, M.; Naumann, M. Increased tooth mobility because of loss of alveolar bone support: A hazard for zirconia two-unit cantilever resin-bonded FDPs in vitro? *J. Biomed. Mater. Res. B Appl. Biomater.* **2014**, *102*, 244–249. [[CrossRef](#)] [[PubMed](#)]
65. Sinjari, B.; Santilli, M.; D'Addazio, G.; Rexhepi, I.; Gigante, A.; Caputi, S.; Traini, T. Influence of dentine pre-treatment by sandblasting with aluminum oxide in adhesive restorations. An in vitro study. *Materials* **2020**, *13*, 3026. [[CrossRef](#)] [[PubMed](#)]
66. Braga, R.R.; Meira, J.B.; Boaro, L.C.; Xavier, T.A. Adhesion to tooth structure: A critical review of “macro” test methods. *Dent. Mater.* **2010**, *26*, e38–e49. [[CrossRef](#)] [[PubMed](#)]